PID: 1046

Analytical Studies on Auxiliary Box in Composite Fin of Civil Aircraft and Validation of Structural Design by Optimization

Polagangu James
Senior Scientist

Prashob. E
M. Tech Project Student-Amrita School of Engineering-Coimbatore

Byji Varughese
Principal Scientist

Advanced Composites Division
CSIR-National Aerospace Laboratories
Kodihalli, Bangalore
Pin: 560017, India
james@nal.res.in

ABSTRACT

A need is aroused in recent days for a separate space to house the actuators of control surface of wing and empennage structures of civil aircraft. The creation of an independent space outside main structural box is understood as auxiliary box structure. The space for auxiliary box is created by providing an auxiliary spar member between front and rear spars. This auxiliary spar is provided based on technical evidence that mere provision of spar should not make main structural box to reduce its bending stiffness and torsional rigidity. Various analytical studies have been carried out to find the optimum location of spars that resulted in least displacement with least possible mass of the fin structure. The present studies have been carried out on a composite fin structure of civil aircraft which had been previously designed for a given loading and geometry through classical approach. The structural optimization also carried out on a few fin models to see the difference in the mass obtained from structural optimization with that of mass of initial design. It is seen that there is good agreement between optimized mass and that mass of initial design through classical method.

Keywords: Auxiliary box, Civil Aircraft, Composite Fin, Optimization, Stress Analysis

Nomenclature

B_1 Width of the fin at root
B_2 Width of the fin at tip
H Height of fin
f_1 A factors made at root of fin in the load diagram
f_2 A factors made at tip of fin in the load diagram
p_o initially assumed pressure distribution
S Allowable shear strength of the lamina
X Strength of the lamina in the fiber direction,
σ_{11} *Tensile stress from applied load*
τ_{12} *Shear stress from applied load*

1. Introduction

There is very less technical content in literature available on the subject under discussion. Aircraft from different manufactures are seen with auxiliary box provide in the wing, fin and horizontal stabilizers structures. The details on particular aircraft have been obtained from open literature available in the electronics media. However, the authors also believed that the information is trustworthy from the point of view of provision of auxiliary box structure. There are a few transport aircraft provided with the auxiliary box structure irrespective of its size. This supports the need of provision of an auxiliary box that house the actuators operating lifting surfaces. The preliminary structural design on the composite fin has previously been completed prior to initiation of present study. The initial design of composite fin carried out based on theoretical optimization method developed by the organization for composite structure. This can be applied for any airfoil irrespective of wing, Empennage structure including its control surfaces in general. However, this method invokes the involvement of structural designer to have proper control in handling right input and compilation of output data from an excel spread sheet. However, this method has provided a strong

technical evidence for choosing initial thickness for composite fin. This paper however not emphasized the procedure developed for theoretical optimization, but to understand the behavior of composite fin structure of transport aircraft with different position of spars that create required size of auxiliary box structure. And comparison of mass obtained from optimization tool with that of mass from initial design is made.

2. Objective

The objective of this study is to work out the location of front, rear spar and auxiliary spar location in composite fin structure of civil transport aircraft using analytical approach. And choose the fin configuration that is stiff and rigid. Compare the mass of initial design with that mass obtained from structural optimization.

3. Motivation

The wing, vertical and horizontal tail are generally attached with respective control surface like flaps, aileron, rudder and elevators. These control surfaces are operated by actuators mounted within the torque box of primary load carrying members. The cutouts are introduced in the skin members to ease the installation, regular maintenance and repair of actuators. Introduction of these cutouts in the skin members which is main load carrying member may results in higher thickness of skin around cutout by reinforcing the weaker region. It also demands fasteners for connecting access cover plates to these cutouts, thereby increasing the weight of overall structure. Besides, this frequent removal of access covers and fasteners connected to it, may pose severe problems around holes in the skin member which is main bending load carrier. The composite skins of co-cured and/or co-bonded structures, any damage in skin at a local region may results in discard of complete skin member irrespective of size of component, unless proper repair technology is developed and made available for in-situ repairs. It ultimately leads into a situation of loss of money, time and labour. Therefore, provision of auxiliary box for housing the actuators helps to eliminate the frequent removal and the problem associated with such frequent removal.

4. Geometrical details of fin

The vertical stabilizer of civil and transport aircraft is usually made up of two-spar, skin-stringer construction with multi inter-spar ribs that always results in least mass over multi-spar construction. Design of fin structure with multi-spar construction is acceptable for combat aircraft as it is mission orientated, not business similar to civil and transport aircraft. Therefore, the option of multi-spar construction of composite fin of civil aircraft is ruled out. The present study considered the fin with two spars with monocoque skin construction as depicted in Fig. 1. The inter-spar ribs are placed perpendicular to the rear spar for most of ribs except those that are placed at root section.

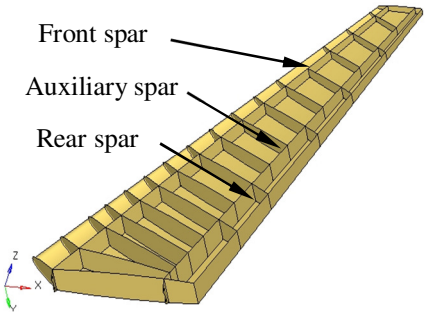

Fig. 1 NMG of fin considered for the study (Top skin is removed for better view)

5. Load on fin

The critical design load for design of fin structure is found to be from Gust load case. Generally airfoils are subjected to uniformly varying distributed pressure load for any type of maneuvering. Similar type of loading is assumed for the present analytical studies. The intensity of pressure load distribution is assumed to be around 1 T/m^2 for civil and transport aircraft which is obtained from previous programs at CSIR-National Aerospace Laboratories-Bangalore. The similar assumptions are also made in this work with forward center of pressure case. The absolute values of pressure intensity acting at various rib location has been arrived at based on span-wise triangular variation from root to tip while maintaining maximum intensity at root location. The chord wise variation has been arrived at based on assumption that the peak pressure at leading edge and zero pressure at trailing edge. These assumptions are made in absence of aeroelasticity load data, as 95% of solutions to many engineering problems can be obtained by making an appropriate assumption and the rest 5% of the solution may be verified for its correctness as and when actual data is available.

The mathematical calculations are discussed in details in this paper as this kind of approximation in pressure variation for the first time envisaged and adopted by the Empennage of group of National Civil Aircraft program. However, these assumptions are proved to be in agreement with the load distribution obtained from static aeroelasticity when looked at gross load on fin structure. However, the much of analytical work has prior been carried out with the assumed load distribution therefore discussed in detailed as given below. The present analytical studies did not consider rudder in its place and reaction load from rudder also not considered as the solution obtained through this study forms the guideline to choose the position of spar location for a given load and geometry of fin. The sizing of all

structural components of fin of course requires complete details from rudder from its structural details to reaction force. Similar load distribution may be assumed even if, rudder is in its place. The assumption made in the load distribution is still valid provided the geometrical details are taken into account from leading edge of fin to the trialing edge of the rudder.

5.1. Initial loading distribution

Initially it has been assumed that a uniform pressure p_o (1 T/m^2) is acting through the surface on left skin of the fin structure as shown in Fig. 2. It indicates that whole fin structure from root to tip and leading edge to rear spar is subjected to a uniform pressure distribution. The value of intensity of pressure is same at all four corners of the loading diagram.

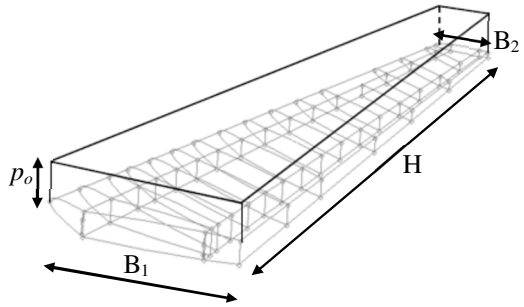

Fig. 2 initially assumed pressure distribution.

5.2. Chord correction to load distribution

A second assumption has been made with respect to the chord of airfoil. The uniform pressure of p_o has been converted into equal triangular load distribution with zero pressure along rear spar and along the leading edge of airfoil it is $2p_o$as shown in Fig. 3. The area of loading diagram is unaltered with this assumption.

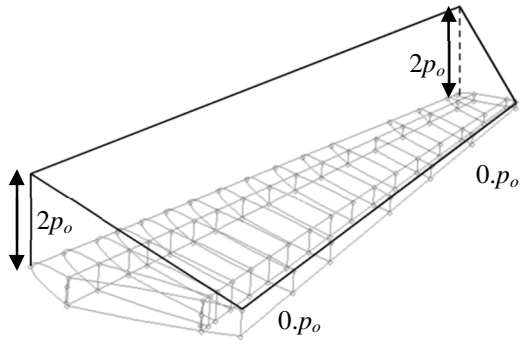

Fig. 3 Pressure distribution after chord wise correction

5.3. Span correction to load distribution

The third assumption is made with respect to the span of airfoil based on the pressure diagram worked out in previous steps. The triangular variation distribution that is shown in Fig. 3, now subjected to further correction with factors f_1 and f_2 which depends on the chord width B_1 and B_2 at root and tip respectively. The correction in the loading diagram made with respect to chord width resulted in pressure diagram shown in Fig. 4. After this correction, the pressure intensity is more at the root and less at the tip than that is mentioned in Fig. 3. These correction factors are given in *Eq-(1)* at the root and tip of fin respectively.

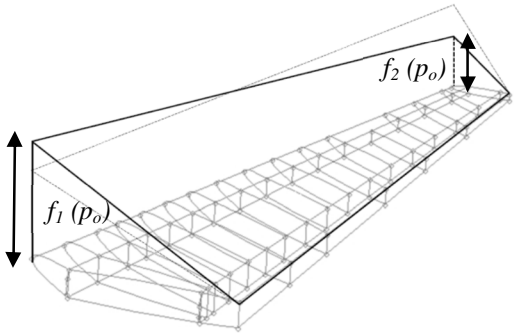

Fig. 4 Final pressure distribution after span wise correction

$$f_1 = \left(2 + \frac{B_1}{B_2}\right), \quad f_1 = \left(2 - \frac{B_2}{B_1}\right) \qquad \text{Eq-(1)}$$

The additional magnitude of pressure load over and above $2p_o$acting along the leading edge of airfoil at each rib location can be obtained by using X. Tan (θ_2).Where X, is the point along height of the fin originating from tip end ranging from 0 to H. The pressure load acting along the leading edge at all ribs are calculated as given in Table 1.

Table 1 Calculated pressure values of ribs

Ribs	Pressure, MPa	Ribs	Pressure, MPa
Rib - 1	0.06153	Rib - 9	0.04060
Rib - 2	0.05816	Rib - 10	0.03794
Rib - 3	0.05479	Rib - 11	0.03527
Rib - 4	0.05289	Rib - 12	0.03260
Rib - 5	0.05058	Rib - 13	0.02983
Rib - 6	0.04826	Rib - 14	0.02707
Rib - 7	0.04594	Rib - 15	0.02430
Rib - 8	0.04327	Rib - 16	0.02153

6. Initial sizing of composite members

For above loading diagram, the initial sizing of all composite structural components of fin has been evaluated by classical method using modified Yamada Sun's failure criterion given in *Eq-(2).*

$$FI = \sqrt{\left(\frac{\sigma_{12}}{X}\right)^2 + \left(\frac{\tau_{12}}{S}\right)^2} < 1.00 \qquad \textit{Eq-(2)}$$

Instead of freezing the thickness of all composite at once, a theoretical optimization procedure has been developed for this program by using which a fair and accurate thickness and stacking sequence of skin and spars members have been arrived at as given in Table A1 to Table A4 in Appendix. The stacking sequence and thickness are used for carrying out finite element analysis with different spacing of spar location to find out optimums positions of spars. The details of finite element analysis are discussed below while emphasizing more on results and trends observed.

7. Number of FE model considered

The Numerical Master Geometry have been created for different positions of front and auxiliary spar while maintaining rear spar location same for all models. The various positions of front and auxiliary spars are defined in terms of constant percentage of chord at root and tip as given in Table 2. The structural analytical study has been carried out on these models. The initial sizing of composite fin structures was completed for the model with front spar location at 12% and rear spar location at 70% with no auxiliary spar in place.

Table 2 Spar positions details

S. No	Location of spars
1	FS at 12% &IS at 50%
2	FS at 12% &IS at 55%
3	FS at 15% &IS at 50%
4	FS at 15% &IS at 55%
5	FS at 18% &IS at 50%
6	FS at 18% &IS at 55%

8. Finite element analysis

The step wise procedure followed for carrying out finite element analysis is explained below.

8.1. FE modeling

A brief summary on finite element analysis is provided on the composite fin structure. The materials used for the analysis are given in Table 3.

Table 3 Properties of composite and metal materials

S. No	Propert	Composit	Aluminum
01	E_1	1.3 E+05	7.20E+05
02	E_2	1.0 E+04	-
03	ν_{12}	0.35	0.33
04	G_{12}	5000	-
05	ρ	1.70E-06	2.80E-06
06	t	0.15	-
07	X_t	432	-
08	X_c	506	-
09	Y_t	25	-
10	Y_c	25	-
11	S	36	-

Composite material: T300 Graphite /epoxy, metal Al alloy, Unit: mm, MPa, Kg/mm^3

The PCOM properties with MAT8 material cards are used. The details of thickness and stacking sequence of all composite components are modeled by using the information given in Table A1 to Table A4 in Appendix. The finite element models for the six models of composite fin structures have been modeled using HYPERMESH® tool as pre-processor. The average size of element chosen is around 25 mm x25 mm as to eliminate the issues of convergence and with an intension of using the same model for carrying out buckling analysis. All models are divided in to finite element by using CQUAD4 and limited CTRIA3 elements of NASTRAN® as shown in Fig. 5. The loading discussed in above section are applied at appropriate rib location on fin model and interpolated in between adjacent ribs.

Fig. 5 Finite element modeling of fin structure

Proper checks have been made to see that the loading on models is applied in accordance with the theoretical estimation as shown in Table 4. The applied uniformly varying load distribution is shown in Fig. 6.

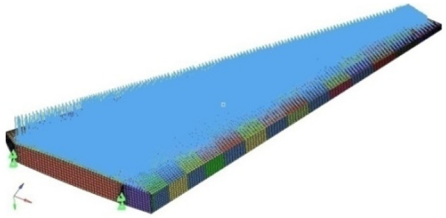

Fig. 6 Uniformly varied distributed load on fin

The difference in load obtained from theoretical estimation and applied load on finite element models found to be in well agreement as seen in Table 4. There are only two fin to fuselage fittings considered for this study that can resists bending in Z-direction and shear in Y-direction. These two fittings are constrained against all translation against x, y and z direction on either side of fin as shown in Fig. 7. The plane of fittings is parallel to YZ plane.

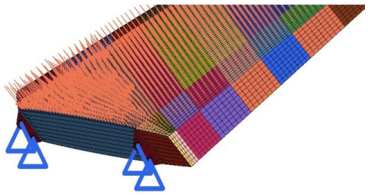

All points are constrained against Δ_x, Δ_y, Δ_z=0

Fig. 7 Constraint applied at fittings of fin

Table 4 Comparison of theoretical and applied load on FE models

Model name	Theoretical estimation of load	Load on FE model	% of deviation
Model 1	178680	178463	1.00
Model 2	178680	179575	0.99
Model 3	178680	180797	0.98
Model 4	178680	168323	1.06
Model 5	178680	168778	1.05
Model 6	178680	156823	1.14

Unit, N

8.2. Mass and displacement

From the results of structural analysis carried out on all FE models of fin, the model with highest stiffness and low mass is identified. The displacement and mass of each model has been compared as shown in Table 5 and Fig. 8.

Table 5 Statement on mass and displacement

Model No	Max. Displacement (mm)	Total Mass (Kg)
Model 1	139	309.251
Model 2	136	315.351
Model 3	135	301.631
Model 4	131	308.731
Model 5	110	291.473
Model 6	115	296.773

It has been observed that the displacement of FE model increases as the mass decreases. However, the displacement of model-5 decreased even though the mass of FE model increased linearly, which is due to the fact that the torsion effect on box decreased as the center of pressure almost located near the shear center of the box. In model-6, the center of pressure and shear center moved away, that resulted in little higher displacement.

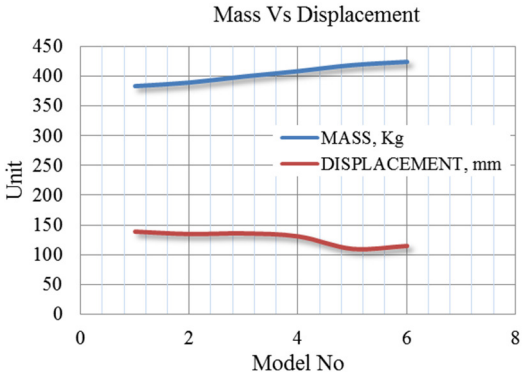

Fig. 8 Mass Vs Displacement

The subject on the center of pressure and shear center is not discussed in detail in this paper. The optimum location of spars that resulted in high stiffness with least mass is identified. It is understood that the fin with structural configuration of model-1 and model-5 have to be understood further by carrying out detailed analysis. These two models showed high mass with least displacement and least mass with high displacement. It can be concluded that the highest structural performance model is obtained for the fin model with the spar positioning at front spar at 18% & Intermediate spar at 50% of chord length as explained in Table 2.

8.3. Reaction in fittings

The reaction along global x, y and z axes are extracted at each lug of both front and rear fittings. The reaction component acting along X, Y and Z-axes are shown in Fig. 9 to Fig. 11respectively.

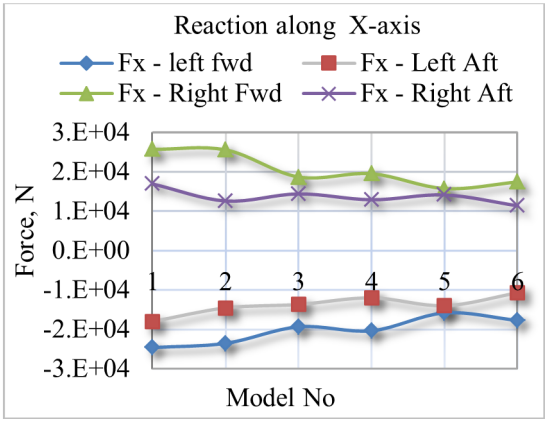

Fig. 9 Reaction along X-axis

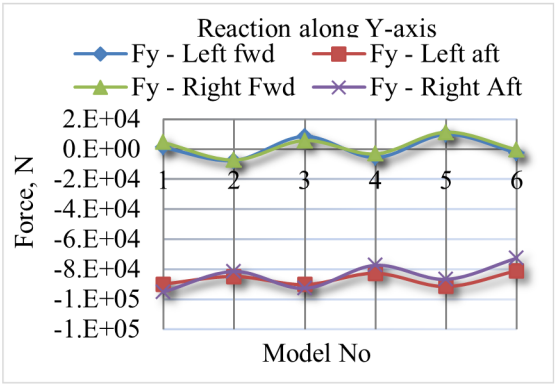

Fig. 10 Reaction along Y-axis

The reaction force along X-axis reduces as the position of front spar and rear spar moves towards trailing edge in general. For a given position of front spar, shifting of rear spar towards trailing edge resulted in higher values of reaction in forward lugs (front fitting) and reduced in aft lugs (rear fitting). The reaction force along Y-axis increased as the position of front spar and rear spar moves towards trailing edge in general. For a given position of front spar, shifting of rear spar towards trailing edge

resulted in higher values of reaction in forward lugs (front fitting) and reduced in aft lugs (rear fitting).

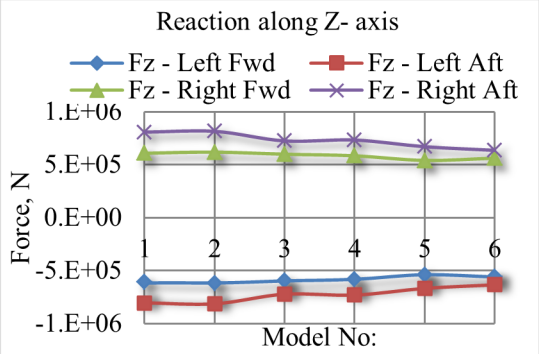

Fig. 11 Reaction along Z-axis

The reaction force along Y-axis increased as the position of front spar and rear spar moves towards trailing edge in general. For a given position of front spar, shifting of rear spar towards trailing edge resulted in lower values of reaction in forward lugs (front fitting) and increased in aft lugs (rear fitting). This has happened due to movement of spars towards and way from center of pressure. The reaction along Z-axis reduces as the position of front spar and rear spar moves towards trailing edge in general. For a given position of front spar, shifting of rear spar towards trailing edge resulted in lower values of reaction in forward lugs (front fitting) and similar trend is observed in aft lugs (rear fitting). This has happened due to increase in the thickness of airfoil / lever arm between left and right lugs.

8.4. Buckling Analysis

Stability analysis has been carried out on fin structure with initial layup sequence with the loading and boundary conditions discussed above. It has been found that the skin member that is subjected to compressive stress (right hand skin) has failed in buckling with first Eigen values of 0.97 as shown in Fig. 12.

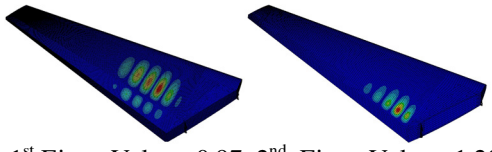

1st Eigen Value =0.97 2nd Eigen Value =1.20

Fig. 12 Buckling modes

The composite fin structure is safe from its stability point of view from second buckling mode onwards as the second Eigen values is found to be above 1.00 (1.20). Then the stacking sequence of skin members in the region of failure has been modified suitably by increasing number layers from 56 to 80 numbers with an additional plies of required orientation, while maintaining the percentage of 0^o plies within 30-40%, $\pm 45^o$ plies within 40-50% and 90^o plies within 10-12% of total number of plies. The initial stacking sequence of skin members failed in buckling due to the fact the theoretical optimization had been carried out for the load distribution shown in Fig. 2 where the effect of torsion is not accounted due to varied load distribution across the chord. After modification skin members locally the Eigen values have been extracted for first 10 modes with an intension of showing the smooth variation of Eigen values when read from first mode to the tenth mode as given in Table 6.

Table 6 Eigen values for modified layup sequence

M No	M-1	M- 2	M– 3	M- 4	M- 5	M- 6
1	1.24	1.666	1.226	1.910	1.511	1.50
2	1.297	1.668	1.256	1.980	1.607	1.54
3	1.36	1.670	1.300	2.203	1.647	1.81
4	1.434	1.695	1.348	2.415	1.699	1.99
5	1.444	1.895	1.407	2.431	1.708	2.04
6	1.532	1.998	1.484	2.486	1.783	2.13
7	1.574	2.074	1.512	2.488	1.940	2.37
8	1.597	2.141	1.536	2.611	1.998	2.41
9	1.613	2.172	1.579	2.676	2.020	2.50
10	1.671	2.299	1.614	2.680	2.069	2.52
Mass	309	315	302	309	291	297

Note: M-Model, Mass in Kg

This smooth variation of Eigen values indicates that the uniform distribution of mass in the composite fin structure, which proves that the base structural design, is acceptable in absence of analytical tools. The mass of finite element models of all fin models after modification of stacking sequence are marked in the same table. This mass includes only skin members, three spars, and all ribs. The mass of nose box is not considered as not much work has been initiated to arrive at the minimum thickness required for nose skin from the bird impact regulations.

8.5. Strength Analysis

Failure Index analysis [2] provides the information about plies which fail under given loading condition. In many practical cases, the residual strength of a laminated composite part after the first-ply-failure (FPF) is still high enough to prevent the rupture of a component. So applying FPF criteria for the design may lead to conservative sizing. This is not desirable in high performance applications where the weight penalty is a serious concern from operation point of view. Failure Index Analysis (FIA) allows engineers to examine structural behavior beyond first ply failure (FPF) and understand post FPF events of the composite material in the nonlinear field. However, the present study restricted to only FPF theory as the thickness of each composite members have been wisely chosen based on technical evidence. The strength of laminate after first ply failure is not considered as the residual strength

available in the laminate, as at most care has been taken by the initial designer of the composite fin structure while arriving at the initial sizing of all structural components.

The modified Yamada Sun's failure criterion has been used for predicting failure index values in each lamina in the laminate of skin, spars, and rib components available in fin structure of all finite element models. The failure index values at the root and away from the root section of fin are given in Table 7. The region where the failure index values more than 1.00 at the root section is due to the fact that the skin members, spars and root rib have not been sized for the heavy concentrated loads acting in the fitting locations. Therefore failure of the section at the root location can be ignore in this study. The composite components away from root section found to be safe in strength as the failure index value is less than 1.00.

Table 7 Failure index values in the fin at root and away from the root section

Name	Left Skin		Right Skin		Rib & Spar	
	At root	Away from root	At root	Away from root	At root	Away from root
M-1	1.88	0.85	1.64	0.82	3.06	0.98
M-2	1.68	0.89	1.38	0.73	2.76	0.96
M-3	1.37	0.96	1.18	0.65	2.63	0.89
M-4	1.61	0.76	1.22	0.61	2.47	0.86
M-5	1.12	0.59	0.96	0.52	1.91	0.78
M-6	1.19	0.61	1.15	0.55	1.95	0.70

M-Model

9. Optimization

Before proceed with structural optimization on inter-spar box of composite fin, an attempt is made to understand the effect of initial sizing on mass obtained from optimization. The following section describe the effect of initial sizing, mass constrained on final mass converged from optimization methods.

9.1. Impact of initial sizing on optimization

The aim of performing initial structural design prior to carry out structural optimization is that the initial thickness of each ply defined as initial thickness of a given ply in optimization influences the final thickness of that particular ply orientation or laminates as a total. Therefore, it is an important to note that the optimization of any structure should be performed after completion of preliminary structural design based on classical engineering methods. Otherwise the results obtained from optimization tools tend to mislead the analyst as well structural designer. However, the optimization is not denunciated completely as certain information still can be obtained while understanding trends not the exact thickness of any structural components. A case study has been undertaken to demonstrate the fact that the initial thickness defined in optimization deck influence the final thickness arrived at from optimization as discussed in below.

9.1.1. A case study to show the effect

The details of finite element modeling considered for studying the effect of initial mass and final mass are discussed in this section. The study is carried out on a rectangular plate of 200 mm x 100 mm size subjected to total compressive load of 100 N at one end, constrained against all translations and rotation at other end as shown in Fig. 13.

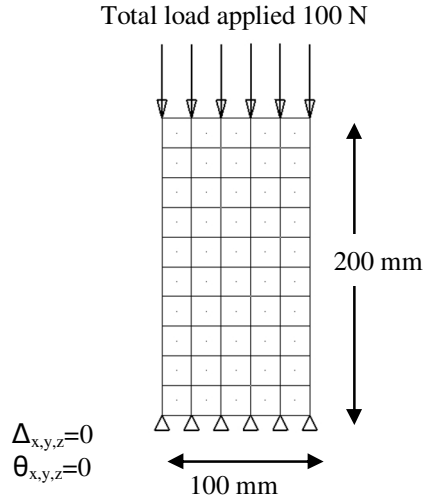

Fig. 13 FE model used for studying the effect of initial mass and final mass from optimization

The modeling is carried out with regular 4 node 2D elements of 20 mm x 20 mm size, which is converged size of element for the size of geometry considered. The optimization has been carried out by using the standard procedure of Optistruct® with failure index <1.00 and Eigen value >1.00 as design constraints and minimum mass as design objective. The optimization is performed using composite materials with base orientation of $(+45,-45, 0, 90)_{sym}$ stacking sequence. Different values of thickness for each ply (1mm, 2mm 4mm) is assumed initially as to create a varied initial mass values. The optimization has been carried out with 0.25 Kg and 0.50 Kg minimum mass as design objective. The converged mass from optimization that satisfies the design constraints failure index and buckling are listed in Table 8. The same variation is depicted in Fig. 14. Upon careful examination of these values, it is understood that the initial mass defined in the optimization deck has an influence on final mass obtained from optimization procedure for any design constraint values of mass. It also conveyed that there exists only one optimum mass for a given structural configuration and system of loading and boundary condition. The problem that has been considered to

demonstrate this effect has got only a single optimum value of mass of 0.0432 Kg, as shown in the Fig. 14. The minimum optimized mass is worked out when the initial mass defined between 1.02-1.54 kg.

Table 8 Initial mass and optimized mass for mass constraint of 0.50 Kg

Initial mass	Min mass cons	Opt mass	Min mass cons	Opt mass
0.26	0.50	5.0E-02	0.25	5.6E-02
0.51	0.50	4.8E-02	0.25	4.8E-02
1.02	0.50	4.3E-02	0.25	4.8E-02
1.54	0.50	4.5E-02	0.25	4.3E-02
2.05	0.50	4.8E-02	0.25	4.8E-02

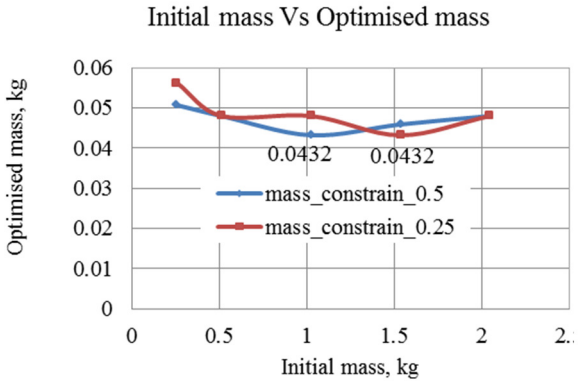

Fig. 14 Initial mass and final mass from

Though there are other optimized mass values available for various initially defined mass values, but that is not minimum possible optimized mass for a given structure and loading. In addition to this fact one more noteworthy point observed is that it is not only initial mass has an influence on optimized mass, but the constrained mass has also showed considerable effect on the optimized mass. With all observation one can understand the importance of working out initial sizing of any structure based on classical engineering methods. No analyst or structural designer should choose the root of optimization without completion of structural design in the beginning. Otherwise, the results obtained from optimization procedure tend to mislead the overall structural design, at the end it may result in catastrophic failure of structure when tested for the designed loading system or may add up extra mass which is uninvited especially in civil transport aircraft. The observation made in this section made the authors to proceed further with optimization only up on completion of initial sizing of all structural components of composite fin. The optimization performed on the composite fin structures are discussed in detail in the following sections.

9.2. Optimization of inter-spar box

In this study only the inter-spar box portion of fin is considered for optimization. For preliminary optimization, FE models -1 and Model-5 with highest mass and displacement have been selected as explained in Table 5. The process expands upon three important and advanced optimization techniques, viz. free sizing optimization, sizing optimization and ply stacking sequence optimization using Optistruct [3].

9.2.1. Problem definition

The same geometry details, elements size, material properties and loading that have been initially used in the above analysis are used in the optimization analysis. The inter spar box of fin consisting of skin members, spars, ribs are modeled with four ply basic orientations (0°, 45°, -45°and 90°) with a uniform initial thickness of 2 mm. The SMEAR option is applied in the PCOMP card to eliminate stack biasing. The fin has been designed on considering two major performance criterions such as the minimum displacement, and minimum mass. The following optimization setups are defined in the optimization phase to identify the stiffest design for the given fraction of the material. The manufacturing constraints are also incorporated in the process of optimization. The objective function in this problem is to minimize the mass of fin structure by taking weighted compliance into consideration with design constraints buckling factor > 1 and failure index values < 1. The structural optimization on the inter-spar box of fin has been carried out based on the following formulation and definition, various conditions and manufacturing constraints are considered and defined in the concept design. The manufacturing constraints such as ply percentage for the 0^s and 90^s such that not less than 10% and nor more than 60% exist. The equivalent ply thickness after manufacturing is 0.15. The balance of plies constraint that ensures an equal thickness distribution for $\pm 45^s$ also defined. The free sizing, size optimization and ply shuffling steps have been performed as per standard procedure defined in the Optistruct® optimization procedure, therefore, not discussed in detail in this paper. The size optimization has been carried out with one more added design objective function displacement should not be more than 110 mm as it is depicted in Table 5. The optimization has been completed within third iteration as the initial input thickness are given in such a way that it is very near to the optimum solution of the problem. The mass obtained from optimization after satisfying all design constraints, objective functions are given in Table 9, with root section and without root section before optimization and after optimization. It has been observed that the thickness of left and right skin members are different as seen from column 5, 6 of the same table.

Table 9 Optimized mass of all components of fin with and without root section

S.N	Design variable	Model 1 , Mass (kg)			
		Before optimization		After optimization	
		With root	*No root*	*With root*	*No root*
1	*2*	*3*	*4*	*5*	*6*
1	Left skin	107	96	99 (121)†	94 (115)†
2	Right skin	107	96	121	115
3	Front spar	18	18	18	19
4	Aux. spar	22	22	33	31
5	Rear spar	19	20	15	14
6	Fin rib	56	57	33	39
7	Aux rib	23	23	8	11
	Total	352	335	327 (349)#	324 (345)#
Model 5 , Mass (kg)					
1	Left skin	98	84	76 (109)†	72 (90)†
2	Right skin	98	84	109	90
3	Front spar	18	16	15	12
4	Aux. spar	22	22	37	35
5	Rear spar	18	18	13	13
6	Fin rib	52	50	48	47
7	Aux rib	22	21	21	19
	Total	329	294	320 (353)#	288 (305)#

† Maximum mass of left or right skin member from buckling consideration

 # Total mass of fin considering maximum thickness of left or right skin members that accounts symmetry about aircraft center line

This has occurred due to the fact that the load has been applied on left side of the fin that makes the right skin members driven by buckling criterion rather than strength. In practice the thickness of left and right skin members should be the same as the fin structure is symmetry about center line of aircraft. The statements of mass, along with the displacement from initial design and optimization have are also reported in Table 10. The least displacement is observed for model-1 whether considered full root section or not. In the initial design the root section has been considered even though this thickness at this section not designed for heavy concentrated loads from fin fuselage fittings. Therefore, it is appropriate to consider the initial design with optimized design for fin model-1. The difference in both mass is shown around 5-12%. Had the initial design been consider stability criterion into effect this difference would have further been reduced. This is the area the initial design should be improved, so as to minimize the difference between initial and optimization solutions.

10. Conclusion

The parametric study to work out the location of front, rear spar and auxiliary spar locations in composite fin structure of civil transport aircraft using finite element analysis approach is carried out. Varieties of analytical studies with different location of spars have been carried out to identify the optimum location of spars. The structural configuration that has resulted in least displacement at the tip of fin with least mass is considered as an optimum location of spar to create auxiliary box. The structural configuration of model-1 has met this criterion, therefore found to be suitable for continuing many more studies on this model**.** The optimized mass from preliminary structural optimization has showed that the mass from its initial design is in agreement within 5-12%. It indicates the initial design of all finite element models should first be carried out using classical methods and then continued with structural optimization as to have proper control on outcome of optimization results. Otherwise, the outcome from optimization may mislead the designer and analysts while selecting the best structural configuration.

11. Future work

The present study considered the load with only forward center of pressure. The further studies should be continued with mid center of pressure and aft center pressure, which are also critical loading conditions for design of any airfoil. It is recommended to continue the further studies by considering rudder attached to the fin structure as it may completely simulate the stiffness of both fin and rudder together on the structural behavior of fin.

Table 10 Statement of mass and displacement from optimization

Case	Fin Model	Weight (kg)		Displacement (mm)		Deviation in initial design and optimized in %
		Initial design	Optimized	Initial	Optimized	
Without Root Box	M-1	262	324 (345)#	77	105	23.62-31.51
	M-5	249	288 (305)#	81	105	15.69-22.91
Full Box	M-1	309	327 (349)#	77	103	5.65-12.88 †
	M-5	291	320 (353)#	81	104	9.91-21.27

(†) The preliminary design had earlier been carried out on only model-1. The least difference between initial mass and optimized mass is attributed to completion of initial design prior to optimization that has helped to define mass constrain limits during process of optimization.

Acknowledgement

Authors thank Mr. Shyam Chetty, Director of CSIR-National Aerospace Laboratories, and Mr. H. N. Sudheendra, Head of Advanced Composites Division for extending finance and administrative support.

References

Books

[1]. NASTRAN manuals

[2]. Robert M Jones "Mechanics of composites Materials", Second Edition, April 1999, Taylor & Francis Inc., Philadelphia

[3]. Optistruct optimization manual

Appendix

Table A1 Stacking sequence of skin member

No of plies, t	Ply sequence
8,1.20	(45,-45,0,90)/sym
10,1.50	(45,-45,0,45,-45,0)/sym
14,2.10	(45,-45,0,90, 45,-45,0)/sym
18,2.70	(45,-45,0,0,90, 45,-45,0,0,90)/sym
20,3.00	(45,-45,-45,0,45,0,90, 45,-45,45)/sym
22,3.30	(45,-45,0,-45,0,45,0,90,45,-45,45)/sym
24,3.60	(45,-45,0,0,-45,0,45,0,90, 45,-45,45)/sym
26,3.90	(45,-45,0,90,0,-45,0,45,0,90, 45,-45,45)/sym
28,4.20	(45,-45,0,90,0,-45,0,45,0,0,90, 45,-45,45)/sym
32,4.80	(45,-45,0,90,-45,0,-45,0,45,0,0,90, 45,-45,0,90)/sym
34,5.10	(45,-45,0,90,-45,0,-45,0,45,0,45,0,90,45,-45,0,90)/sym
38,5.70	(45,-45,0,90,-45,0,-45,0,45,0,90,45,0,90,45,-45,0,90)/sym
46,6.90	(45,-45,0,90,-45,45,0,-45,0,-45,45,0,90,45,0,90, 45,-45,45,0)/sym
52,7.80	(45,-45,0,90,-45,45, 0, -45, 0, 45,-45, 0, 90, 0, 45, 0, 90, 45, -45, 45,0, 45, 0, 90)/sym
62,9.30	(45,-45,0,90,-45,45,0,-45,0,45,0,-45,0,90,0,45,0,90,45,-45,-45, 0, 45, 0, 90, 45, -45, 0, 45, 0, 90)/sym
80,12.00	(45,-45,0,90,0,-45,0,90,45,0,90,0,-45,0,45,0,-45,0,45,0,90,0,-45,0, 45, 0, 90, 45, -45, 45, 0, 45, 0, 90, 45,-45,0,45,0,90)/sym

Table A2 Stacking sequence of inter-spar members

No of ply, t	Ply orientation sequence	Thickness, mm
16,2.40	(45,-45,0,90,-45,45,0,-45,0,45,-	2.4

Table A3 Stacking sequence of stringers

No of ply, t	Ply orientation sequence	Thickness, mm
4,0.60	(45,-45,0,90)/sym	1.20

Table A4 Stacking sequence of all spar members

No. of plies, t	Ply orientation sequence
4, 0.60	(45,-45)/sym
6, 0.90	(45,-45,0)/sym
8, 1.20	(45,-45,0,90)/sym
10, 1.50	(45,-45,0,0,90)/sym
14, 2.10	(45,-45,-45,0,45,0,90)/sym
16, 2.40	(45,-45,0,-45,0,45,0,90)/sym
18, 2.70	(45,-45,0,0,-45,0,45,0,90)/sym
20, 3.00	(45,-45,0,90,0,-45,0,45,0,90)/sym
22, 3.30	(45,-45,0,90,0,-45,0,45,0,0,90)/sym
24, 3.60	(45,-45,0,90,-45,0,-45,0,45,0,0,90)/sym
26, 3.90	(45,-45,0,90,-45,0,-45,0,45,0,45,0,90)/sym
28, 4.20	(45,-45,0,90,-45,0,-45,0,45,0,90,45,0,90)/sym
32, 4.80	(45,-45,0,90,-45,45,0,-45,0,-45,45,0,90,45,0,90)/sym
34, 5.10	(45,-45,0,90,-45,45,0,-45,0,45,-45,0,90,0,45,0,90)/sym
36, 5.40	(45,-45, 0,90,-45,45,0,-45,0,45,0,-45,0,90,0,45,0,90)/sym